Simulation of Asphaltene Aggregation and Related Properties Using an Equilibrium-Based Mathematical Model

ARTICLE *in* ENERGY & FUELS · JULY 2011

Impact Factor: 2.79 · DOI: 10.1021/ef200107k

4 AUTHORS, INCLUDING:

Socrates Acevedo
Central University of Venezuela
111 PUBLICATIONS **1,269** CITATIONS
SEE PROFILE

Manuel Caetano
Central University of Venezuela
32 PUBLICATIONS **338** CITATIONS
SEE PROFILE

María Antonieta Ranaudo
Central University of Venezuela
35 PUBLICATIONS **654** CITATIONS
SEE PROFILE

energy&fuels

ARTICLE

pubs.acs.org/EF

Simulation of Asphaltene Aggregation and Related Properties Using an Equilibrium-Based Mathematical Model

Sócrates Acevedo,* Manuel Caetano, María Antonieta Ranaudo, and Blanca Jaimes

Universidad Central de Venezuela, Facultad de Ciencias, Escuela de Química 40756, Caracas 1053, Venezuela

Supporting Information

ABSTRACT: Aggregation of asphaltenes was simulated using a mathematical model based on the following consecutive equilibrium: $nA \overset{K_1}{\rightleftarrows} A_n$ and $mA + A_n \overset{K_2}{\rightleftarrows} A_{n+m}$, where A, A_n, A_{n+m}, K_1, K_2 represent asphaltenes, n aggregates, $n + m$ aggregates, and equilibrium constants, respectively. A mass balance lead to a $n + m$ polynomial in C (C_0, n, m, K_1, K_2, M), where C is the concentration of free solute (monomer), M is the monomer molecular mass, and C_0 is the total monomer concentration added to solution. Using numerical methods, this polynomial was solved in terms of C_0, K_1, and K_2 for given values of n, m, and M. Selection of $n = 3$, $m = 5$, and $M = 800$ g L^{-1} was consistent with data in the literature, and determination of K_1 and K_2 was achieved by fitting to experimental data from ultrasound velocity, thermal diffusion [thermal lens and dual-beam photothermal reflection (DBPR)], and self-diffusion coefficient techniques. The good fittings found suggest that asphaltene aggregation is adequately described by the present model. A procedure based on the present model was employed to simulate the stepwise adsorption of asphaltenes at the toluene/glass interface. The above sequential equilibrium is discussed in terms of aggregation of the toluene-insoluble asphaltene fraction molecules (A1TM, first equilibrium), followed by incorporation into aggregates of toluene-soluble fraction molecules (A2TM, second equilibrium). This sequential scheme is proposed as a means to keep fraction A1 as nanoaggregates (first step), which, were it not by the presence of A2 (second step), would lead to phase separation. The formation of small aggregates at very low concentrations, predicted by the model, is consistent with the very low solubility of the A1 fraction. When the above mathematical model is combined with the Hansen solubility parameter (HSP) method, it is concluded that asphaltenes form stable colloid solutions in toluene and similar solvents where A1 is insoluble. In other words, for these colloidal solutions, interfacial tension would be zero.

INTRODUCTION

Asphaltene aggregation is a very important property of this sample because of the negative impact that it has in both characterization of the sample and related phenomena, such as colloid flocculation and sedimentation. Aggregation is mainly driven by van der Waals, polar, and hydrogen-bonding interactions. The topic have been extensively reviewed in the literature.[1−3] Molecular aggregates, also called nanoaggregates, are small aggregates whose formation begins at very low concentrations, which is measured in a good solvent, such as toluene. By small, we mean sizes between 1 and 2 nm, and by good solvent, we mean one with a relative energy difference (RED) value less than 1 (see below and the Nomenclature). Dependent upon the technique and conditions used, the formation of molecular aggregates is apparent at concentrations close to 100 mg L^{-1} or less (from here on, unless stated otherwise, conditions will be toluene at room conditions). This has been established by different techniques and different research groups; thus, Sheu et al., using surface tension measurements in pyridine, reported aggregate formation at 0.05 wt %.[4] Acevedo et al. reported aggregate formation close to 90 mg L^{-1}, using a thermal lens technique.[5] Norinaga et al.,[6] using pulse field gradient spin−echo ^{1}H nuclear magnetic resonance (NMR), reported that aggregation would occur at concentrations below 0.1 wt %, and according to self-diffusion coefficient measurements, performed in pyridine, spherical aggregates at infinite dilution would have a hydrodynamic radius of 1.1 nm.[6] Nanoaggregate formation at concentrations close to 0.1 g L^{-1} were reported by Mullins et al. using ultrasound velocities.[7] By a combination of static light scattering, optical absorption, dynamic viscosity, and NMR relaxation measurements, Evdokimov and collaborators[8] studied asphaltene solutions in toluene, reporting an aggregation threshold of 10 mg/L. Lisitza et al.,[9] using ^{1}H NMR spin−echo and diffusion-ordered spectroscopy (DOSY), reported an aggregation onset close to 0.2 g L^{-1} and radii between 1.2 and 3.6 nm for monomers and aggregates.[9] Nanoaggregate diameters close to 2 nm and asphaltene molecular mass in the 500−1000 range were reported using time-resolved fluoresce depolarization (TRFD).[10] Diameters close to 2.5 nm were reported for asphaltene−resin solutions at 250 °C when the freeze-fracture transmission electron microscopy (FF-TEM) technique was employed.[3] Caetano and co-workers, using a dual-beam photothermal reflection (DBPR) method, measured thermal diffusivity coefficients of asphaltenes and found a maximum value close to 0.1 g L^{-1}, consistent with aggregate formation.[11] Quoineaud and co-workers,[12] using DOSY, studied the self-diffusion of asphaltenes from several sources and calculated diameters in the range from 1.3 to about 2 nm, from self-diffusion coefficients extrapolated at infinite dilution.

Received: January 19, 2011
Revised: June 14, 2011

In a series of papers, Acevedo et al. have presented evidence for the presence of two main fractions present in asphaltenes;[13−15] these fractions, called A1 and A2, and the corresponding asphaltenes (As) have the Hansen solubility parameter (HSP)[16] described below, with A1 being practically insoluble in toluene and A2 having solubility properties similar to As.[15] These finding have been found coherent with a colloidal structure model, where periphery is occupied mainly by A2-type molecules (A2TM), whereas A1-type molecules (A1TM) are segregated to the core. As discussed below, these propositions may have an important impact in the aggregation mechanism. Relatively low number average molecular masses (M_n) using vapor pressure osmometry (VPO) close to 1000 g mol^{-1} were reported for A2 solutions of *o*-dichlorobenzene measured at 120 °C.[17] In contrast, A1 afforded higher values (around 2600 g mol^{-1}), emphasizing the strong aggregation tendency of this fraction. M values close to or lower than 1000 g mol^{-1} have been reported using other techniques.[10,18]

In this work, a mathematical model based on two consecutive aggregation equilibrium steps is proposed as a preliminary tool to account for asphaltene aggregation properties. A simulation of several asphaltene experiments was performed to evaluate the plausibility of the proposed model. Multistage aggregation is discussed in terms of the above model and on solubility properties regarding A1 and A2.

EXPERIMENTAL SECTION

Equilibria and Equilibrium Aggregation Constants. We consider the following equilibria for the formation of aggregates:

$$\begin{aligned} &nA \overset{K_1}{\rightleftarrows} A_n \\ &mA + A_n \overset{K_2}{\rightleftarrows} A_{n+m} \end{aligned} \tag{1}$$

In these equations, n and m are number of moles, whereas A, A_n, and A_{m+n} represent single molecules, n aggregates, and $(n + m)$ aggregates of A, respectively; K_1 and K_2 are equilibrium constants defined as follows:

$$K_1 = \frac{C_n}{C^n} \tag{2}$$

$$K_2 = \frac{C_{n+m}}{(C)^m C_n} = \frac{C_{n+m}}{K_1 (C)^{n+m}} \tag{3}$$

In these equations, C values are molar concentrations of corresponding species. Mass balance, in terms of C_0, leads to (see the Supporting Information)

$$C_0 = C + nK_1C^n + (n + m)K_1K_2C^{n+m} \tag{4}$$

where C_0 is the total quantity of asphaltene of molecular mass M added to the solution, C is the equilibrium concentration of non-aggregated asphaltene (molecular mass M), C_n is the aggregate concentration of molecular mass nM, and C_{n+m} is the aggregate concentration of molecular mass $(n + m)M$. These are defined by the following equations:

$$C = f(C_0, n, m, K_1, K_2, M) \tag{5}$$

$$C_n = nK_1C^n \tag{6}$$

$$C_{n+m} = (n + m)K_1K_2C^{n+m} \tag{7}$$

Equation 5 was solved using a numerical program, which gives roots for known values of the argument. In all calculations, values of $n = 3$, $m = 5$, and $M = 800$ were employed. Knowledge of C allows for computation of both C_n and C_{n+m}.

Molar Ratio and Simulations. Here, molar ratios f, f_n, and f_{n+m} are defined by eqs 8−10.

$$f = C/C_0 \tag{8}$$

$$f_n = \frac{C_n}{C_0} = nK_1\frac{C^n}{C_0} \tag{9}$$

$$f_{n+m} = \frac{C_{n+m}}{C_0} = \frac{(n + m)K_1K_2C^{n+m}}{C_0} \tag{10}$$

These definitions are convenient because these ratios are bounded in the 0−1 interval.

Simulation of $\Delta\alpha_{LT}(C_0)$ or the thermal lens heat diffusivity difference was computed using f_n according to eq 11.

$$\Delta\alpha_{LT}(C_0) = af_n \tag{11}$$

In eq 11, a is a scaling constant with the same units as α_{LT}.

Simulation of $\beta_T(C_0)$ or the heat diffusivity corresponding to the dual-beam photothermal reflection (DBPR) method was computed using the following linear combination of f and f_n.

$$\beta_T(C_0) = af + bf_n \tag{12}$$

Here, a and b are fitting parameters with the same units as β_T.

Simulation of self-diffusion constant ratio $D(C_0)$ was computed using eq 13.

$$D(C_0) = \left(\frac{D_S}{D_T}\right)_{C \to 0} f + af_n \tag{13}$$

Here, D_S and D_T are experimental self-diffusion constants measured at infinite dilution, and a is a fitting parameter. Subscripts S and T correspond to sample (asphaltenes) and toluene, respectively.

Ultrasound velocity fitting was carried out using eq 14

$$V_{US} = a + bC_{n+m} \tag{14}$$

where V_{US} is simulated ultrasound velocity, a is the scaling constant, b is a fitting parameter, and C_{n+m} is the aggregate concentration in g L^{-1}.

The procedure to find parameters n, m, K_1, K_2, a, and b in each case could be summarized as follows: (1) Give values to n and m such that the expected size of spherical aggregates is between 1 and 3 nm approximately. For $n = 3$ and $m = 5$, this condition is accomplished and these values were used in all simulations. (2) Use the (n, m) pair to find roots of eq 5 as a function of C_0, K_1, and K_2. (3) Give crude values to K_1 and K_2 such that the slope of curve $C(C_0)$ has a significant drop in the 20−50 mg L^{-1} range. This procedure allows for the determination of K_1 within 1 order of magnitude. (4) Using the above K_1 and K_2 as initial input, search for new pairs to match C_0 corresponding to the maximum of the property being examined ($\Delta\alpha_{LT}$ or β_T). This step allows for the determination of K_2 within about 2 orders of magnitude. (5) Scale simulation to experimental property and search for parameters and refined K_1 and K_2, instructing the fitting program to compute them between appropriated ranges.

Free Energy of the Aggregation Ratio, $\Delta\bar{G}^0_{agg}/RT$. The above total change in free energy of the aggregation ratio per mole of added solute and per liter of toluene was computed from eq 15 (see the Supporting Information).

$$\frac{\Delta\bar{G}^0_{agg}}{RT} = -\frac{\ln[(C_0 + 9.64)^{(n+m)-1}K_1K_2]}{n + m} \tag{15}$$

Here, 9.64 is moles in 1 L of toluene, and $C_0 = 1$ mol. As shown in the Supporting Information, $\Delta\bar{G}^0_{agg}$ could be defined as the standard

dx.doi.org/10.1021/ef200107k |*Energy Fuels* XXXX, XXX, 000–000

Table 1. Parameters Found after Fitting Models to Experimental Data[a]

technique	property[b]	eq	a	b	K_1 ($\times 10^7$, mol^{-2})	K_2 (mol^{-5})	$-\Delta\overline{G}^0_{agg}/RT$[c]
thermal lens	$\Delta\alpha_{LT}$[d]	11	4.4		80	1.00×10^{22}	11
DBPR	β_T[e]	12	0.04	0.47	4	5.00×10^{19}	10
mass diffusion	D_m[f]	13	0.01[g]	0.09	1	4×10^{16}	6
ultrasound	V_{US}[h]	14	1307.0992[i]	0.0677	4	5.00×10^{19}	10
adsorption	ν_{Ad}[j]	22	9	2	5	1×10^{11}	3.2

[a] $R^2 \geq 0.980$ for all fittings. $n = 3$ and $m = 5$ in all cases. [b] Heat and mass diffusion parameters are in $m^2\ s^{-1}$ units. [c] Calculated using eq 15. [d] Thermal lens diffusivity difference. [e] DBPR diffusivity constant. [f] Diffusion ratio (see the text). [g] From ref 12; equal to D_S/D_T; not a fitting parameter. [h] Ultrasonic velocity is in m s^{-1} units. [i] Scaling constant from ref 7; not a fitting parameter. [j] Surface concentration is in g m^{-2} units.

aggregation molar free energy change corresponding to the formation of $n + m$ aggregates from monomers in toluene.

Number Average Molecular Mass, M_n. These were calculated using eq 16 and the K_1 and K_2 values found for the $\beta_T(C_0)$ case.

$$M_n = \frac{\sum_i n_i M_i}{\sum_i n_i} = \frac{M(C + nC_n + (n + m)C_{n+m})}{C_0} \tag{16}$$

In eq 16, M is the molar mass of the monomer.

It is easy to prove that eq 16 has the right limits when $C_0 \rightarrow 0$ and when $C_0 \rightarrow \infty$. In the first case at infinite dilution, only monomer is present, $C \rightarrow C_0$ and $M_n \rightarrow M$. In the second case, $C_{n+m} \rightarrow C_0$ and $M_n \rightarrow (n + m)M$.

Adsorption Simulation. This simulation follows similar lines as the one used above, except that aggregation of aggregates (mimicking flock formation) was employed. First equilibrium is identical to the one in eq 1.

$$nA \overset{K_1'}{\rightleftarrows} A_n \tag{17}$$

Here, we use K_1' to distinguish it from the one above. All equilibria consider here are solution equilibria and do not consider any adsorption as such (see below). Second equilibrium is aggregation of A_n to simulate flock formation in solution.

$$mA_n \overset{K_2'}{\rightleftarrows} A_{n\times m} \tag{18}$$

Here, $A_{n\times m}$ is an aggregate of flock formed by $n \times m$ molecules of A. Using a similar procedure as above, the mass balance equation is

$$C_0 = C + nK_1'C^n + nm(K_1')^m K_2'C^{n\times m} \tag{19}$$

In this case, A_n and $A_{n\times m}$ concentrations are given by eqs 20 and 21, respectively.

$$C_n = nK_1'C^n \tag{20}$$

$$C_{n\times m} = nm(K_1')^m K_2'C^{n\times m} \tag{21}$$

As for other cases above, C was computed using eq 5 and C_n and $C_{n\times m}$ were calculated from eqs 20 and 21, respectively.

Adsorption simulation was computed using eq 22.

$$\nu_C = \frac{aC}{1 + aC} + \frac{bC_{n\times m}}{1 + bC_{n\times m}} \tag{22}$$

In this equation, ν_C simulates the quantity of solute adsorbed per surface unit and quantities a and b are fitting parameters with appropriated units. For reasons to be discussed below, the contribution of A_n was disregarded. Similar to Langmuir-type isotherms, the two terms on the right of eq 22 are self-limited or asymptotic functions; however, in the present treatment, no such isotherm is assumed and adsorption is determined by solution concentration only.

Sizes. The size of the molecule or aggregate was estimated from the density equation using either eq 23 (for spheres) or eq 24 for disks of thickness ε.

$$r = 0.0734\left(\frac{M_J}{\rho}\right)^{1/3} \text{nm} \tag{23}$$

$$r = 0.023\left(\frac{M_J}{\rho\varepsilon}\right)^{1/2} \text{nm} \tag{24}$$

In these equations, r is the radius in nm and M_J is the molecular mass that could be M, nM, $(n + m)M$, or $(n\times m)M$ according to the nature of the species. For calculations, a density of asphaltenes of $\rho = 1.17$ g mol^{-1},[19] monomer $M = 800$ g mol^{-1} (see below), and $\varepsilon = 0.4$ nm[20] were employed.

Solubility Parameters. These were from ref 15 calculated using the sphere program developed by Hansen.[16] Values of D, P, and H correspond to dispersion, polar, and hydrogen-bonding components of HSP. R_0 is the radius of the sphere in the three-dimensional space defined by D, P, and H axes, with the center in the (D, P, H) point corresponding to solubility parameter (SP) components of the sample. Solubility parameter components (D_{n+m}, P_{n+m}, and H_{n+m}) for the octamer aggregate ($n + m = 8$) were calculated using eqs 25.1−25.3.

$$D_{n+m} = \frac{1}{n + m}[(nD_1 + mD_2] \tag{25.1}$$

$$P_{n+m} = \frac{1}{n + m}[(nP_1 + mP_2] \tag{25.2}$$

$$H_{n+m} = \frac{1}{n + m}[(nH_1 + mH_2] \tag{25.3}$$

In these equations, D_1, P_1, and H_1 and D_2, P_2, and H_2 are SP components of fractions A1 and A2, respectively. To obtain these equations, we assumed that the octamer aggregate is composed of n molecules of A1 and m molecules of A2, both with an identical molar volume.

RED values between samples 1 and 2 were obtained using eq 26 as defined by Hansen.[16]

$$\text{RED} = \frac{\sqrt{4(\delta_{D_2} - \delta_{D_1})^2 + (\delta_{P_2} - \delta_{P_1})^2 + (\delta_{H_2} - \delta_{H_1})^2}}{R_0} \tag{26}$$

Here, R_0 is the radius of the sphere with the center at the point (D_2, P_2, H_2), corresponding to SP components of the solute. SP of (D_1, P_1, H_1) corresponds to the solvent or other material whose miscibility with the solute is investigated. Miscibility between the pair is expected for RED < 1.

dx.doi.org/10.1021/ef200107k |Energy Fuels XXXX, XXX, 000–000

RESULTS

Table 1 collects parameters computed in all simulations performed in this work. Mole numbers of $n = 3$ and $m = 5$ were assigned for solving eq 5, which is the first step in all calculations carried out (see the Experimental Section). Selection of these was suggested by reported size particle data for asphaltene nanoaggregates under high and intermediate dilution (see the Introduction). For instance, using $M = 800$ g L^{-1} as the molecular mass, diameters in the 1.3−2.6 nm range are computed for $n = 3$ and $n + m = 8$ for sphere and disk values going from 1.9 ($n = 3$) to 5.4 ($m + n = 8$) nm. The selected M value is coherent with other reported results[10,17,18] (see the Introduction).

In principle, with the same system (asphaltenes in toluene at room conditions), values of K_1 and K_2 should be independent of the method; however, model limitations and differences in asphaltene origin and property examined are likely to lead to differences between these parameters (see Table 1).

In particular, the adsorption case is different from the others because second aggregation is different (compare eq 1 with eqs 17 and 18). The formation of $n \times m$ size particles was used here to simulate flock formation from colloidal n particles or nanoaggregates.

Figure 1 shows the plot c against c_0 using eq 5 to obtain c and fitted K_1 and K_2 parameters shown in Table 1. For Figure 1, we use parameters for fitting β_T (Table 1), although any pair of the four will show that aggregation starts at extremely low c_0.

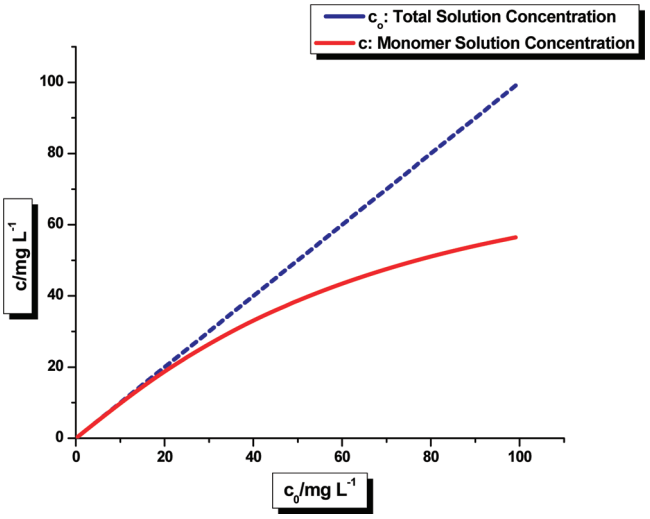

Figure 1. Plot of the monomer concentration c as a function of the total solution concentration c_0. This plot was calculated using eq 5, with $n = 3$, $m = 5$, $K_1 = 4 \times 10^7$, $K_2 = 5 \times 10^{19}$, and $M = 800$ g L^{-1} (see Table 1). These calculation suggest that aggregation begins at extreme low values of c_0 (see the text and Figure 3).

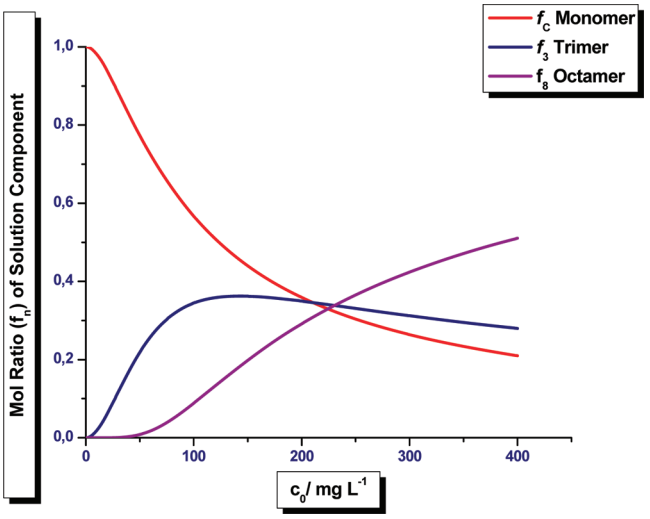

Figure 3. Plot of the mole ratios calculated using eqs 8−10 with parameters used for both β_T and V_{US} simulations (see Table 1). f_3 has a maximum at (143, 0.362). Note that within the present model, the formation of aggregates is a continuous process because aggregates formed are small.

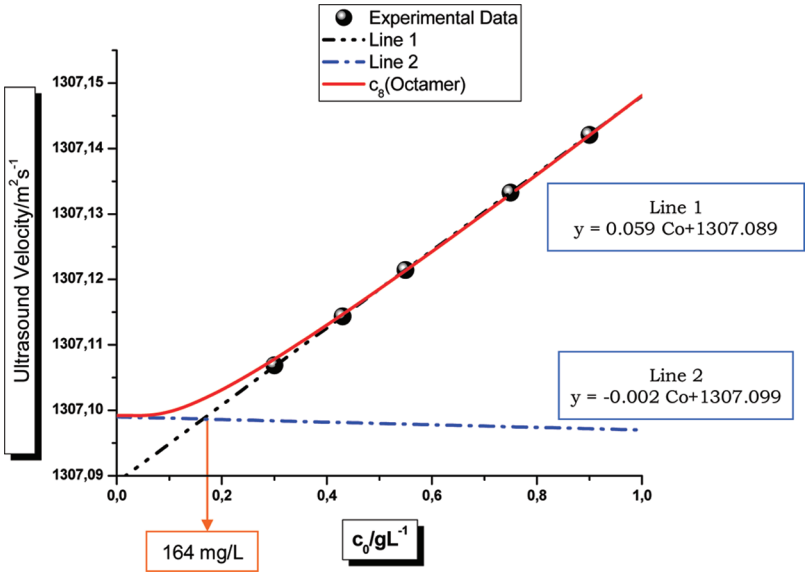

Figure 2. Fitting of eq 14 to reported ultrasound data.[7] The red curve corresponds to c_8 (octamer) as a function of the concentration c_0. Lines 1 and 2 were used for authors[7] to locate the CNAC at the intersection of lines 1 and 2 (164 mg L^{-1}). For fitting, we consider points on line 1 ("experimental data").

dx.doi.org/10.1021/ef200107k |*Energy Fuels* XXXX, XXX, 000–000

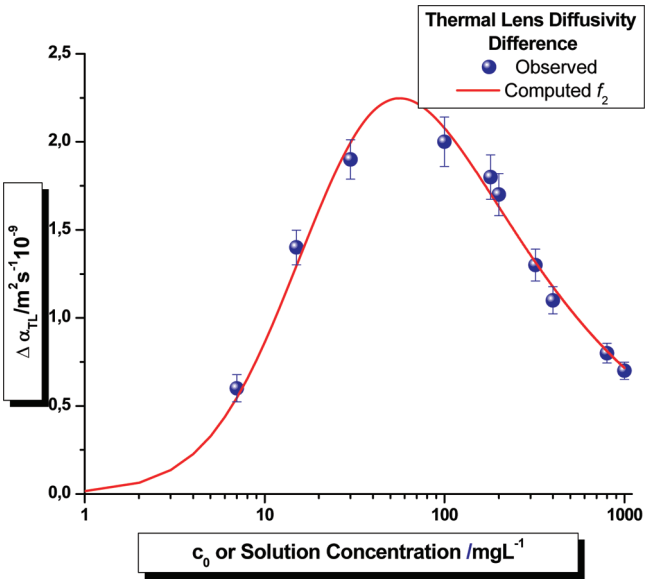

Figure 4. Fitting of eq 11 to $\Delta\alpha_{LT}$ data using parameters shown in Table 1, with a maximum at (56, 2.24). Experimental data are from ref 5.

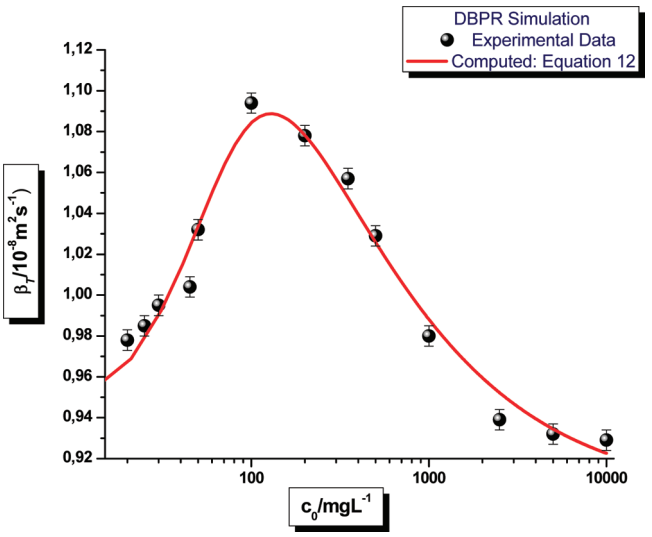

Figure 5. Fitting of eq 12 to β_T experimental data. Calculated maximum are at (129, 1.09). Calculations were performed using parameters shown in Table 1. Experimental data are from ref 11.

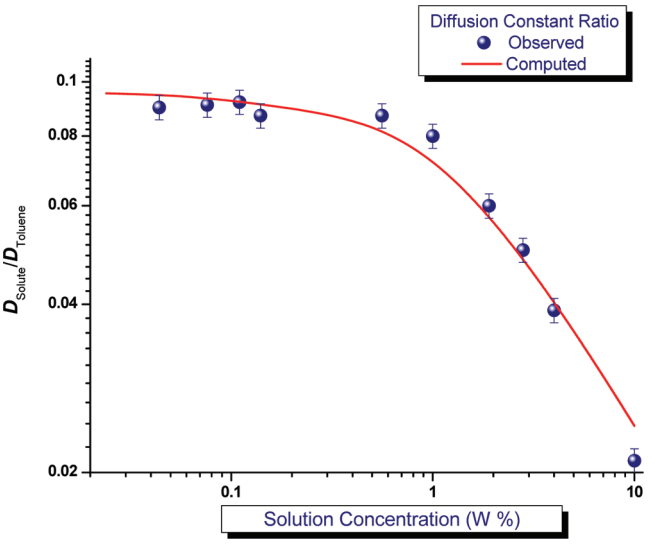

Figure 6. Comparison of the observed diffusion ratio to simulation computed using eq 13, with parameters shown in Table 1. Experimental data are from ref 12.

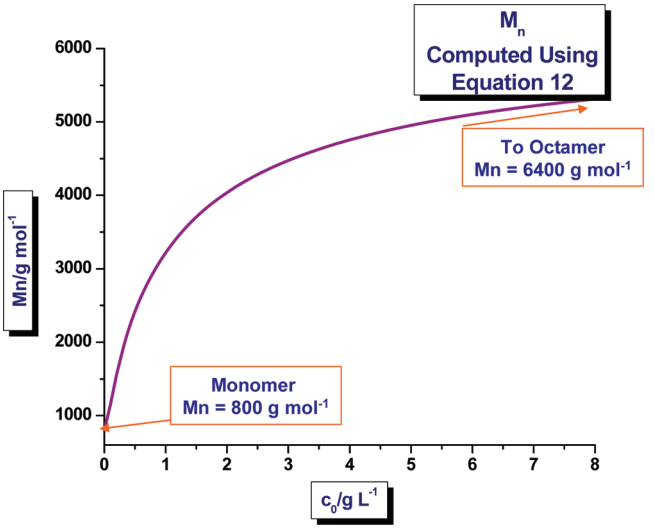

Figure 7. Plot of M_n as a function of c_0 for the mixture of A, A_n, and A_{n+m} computed using eq 16. As shown, the plot has the right M_n limits (800 and 6400 g mol^{-1}).

In Figure 2, fitting of eq 14 to an ultrasound velocity measurement reported by Mullins et al. is shown.[7] A very good fitting (R^2 = 0.997) was found when the c_8 concentration alone was used. As shown here, the critical nanoaggregate concentration (CNAC) is very close to the upsurge of the c_8 concentration at very low c_0 values. Lines shown were used by the authors[7] to locate what they call the CNAC. The main issue regarding Figure 1 is the close resemblance between data and simulation carried out.

Figure 3 shows the change of the mole ratios as a function of c_0. Mole ratios, as defined in eqs 8−10, are convenient because they change in the 0−1 range. These boundaries are very convenient to compare such changes. As expected, f_3 has a maximum because A_3 is the result of opposite effects: the formation by means of equilibrium 1 and consumption by means of equilibrium 2. Note that there is no CNAC, insofar as such a term marks the sudden appearance of aggregates. As shown, the monomer ratio drops continuously with c_0.

Simulation of thermal lens diffusivity difference α_{LT}, using eq 11, is shown in Figure 4. Data for building this are from a previous report.[5] Here, we consider $\Delta\alpha_{LT}$ or the difference between resins and asphaltenes rather than α_{LT} for asphaltenes. Artifacts, likely to be due to absorbance and other optical effects, are apparently discounted in this way. $\Delta\alpha_{LT}$ differences were always ≥ 0 in view of the expected higher mobility of resins. Best fitting parameters are shown in Table 1. For $\Delta\alpha_{LT}$, only f_3 was explicitly considered; however, in view of the above equilibria, both f_C and f_8 are implicitly considered. The same argument stands for all simulations shown in Table 1.

dx.doi.org/10.1021/ef200107k |*Energy Fuels* XXXX, XXX, 000–000

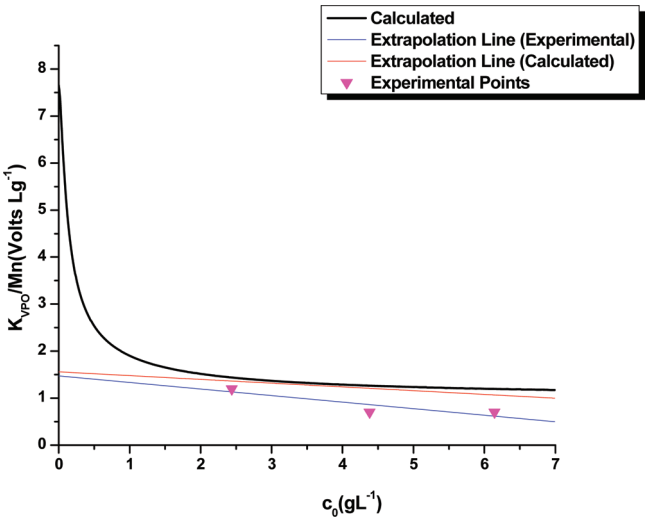

Figure 8. Plot of K_{VPO}/M_n against c_0. Experimental data are from ref 17. The line intersection is equivalent to 4170 g mol^{-1}. The curve intersection is equivalent to M_n = 800 g L^{-1}.

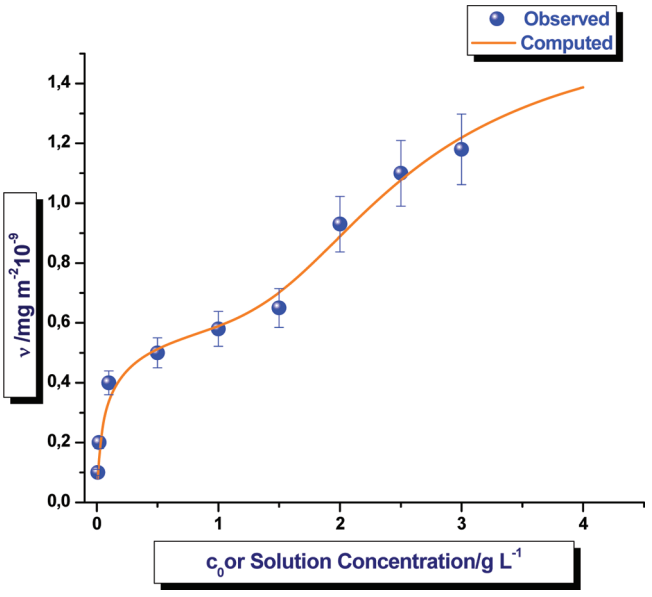

Figure 9. Plot of the adsorbed asphaltenes against c_0 and simulation curve computed using eq 22, with the list of parameters shown in Table 1. Data are from curve c of Figure 4 in ref 19.

Figure 5 shows a simulation corresponding to β_T, using reported data.[11] As was the case for $\Delta\alpha_{LT}$, the dependence with c_0 shows a maximum, a fact coherent with a maximum for f_3 (see Figure 3). As shown in Table 1, the contribution of f_3 to the simulation is 100% for $\Delta\alpha_{LT}$ and 92% for β_T. These maxima and contributions suggest that A_3 is essential within the scope of the present model.

Simulation of the self-diffusion ratio is shown in Figure 6 using eq 13, with parameters shown in Table 1 and data from ref 12. Because both D_{solute} and $D_{toluene}$ extrapolated at infinite dilution were available, we use their ratio as a parameter for f.[12] According to the fitting, the main contribution comes from f_3 or nanoaggregates with n = 3.

Table 2. HSP and RED Values for Samples and Pairs

	SP[a]				
samples and pairs	D	P	H	R_0[a,b]	RED[c]
As	19.5	4.7	4.9	7.3	
A1	20.9	5.6	6.8	7.8	
A2	19.6	5.8	4.4	7.9	
aggregate[d]	20.1	5.7	5.3		
A1−A2				7.8	0.45
aggregate−toluene				7.8	0.87
As−toluene				7.8	0.73
A1−toluene				7.8	1.1
A2−toluene				7.9	0.76

[a] From ref 15 unless stated otherwise. [b] Sphere radius. [c] Calculated using eq 26. [d] SP components for the octamer are calculated using eqs 25.1−25.3.

Figures 7 and 8 show M_n dependence with c_0. M_n values were computed using eq 16. Figure 8 combines computed with experimental data[17] for asphaltenes in toluene measured at 50 °C. Figure 8 is presented in the format employed to analyze VPO results to obtain M_n from a line intercept, in other words, by plotting $\Delta V/c_0 = K_{VPO}/M_n$ against c_0. As shown, extrapolation of experimental points to c = 0 leads to a too high M_n value for the monomer. Moreover, computed values show that more than 90% of the M_n change occurs outside the experimental c_0 concentration range for VPO measurements (≈1−7 g L^{-1}). In view of the low polarity of toluene, these finding are expected. It is interesting that both calculated and experimental extrapolation lines lead to the same intercept, supporting the plausibility of the model.

Simulation of the adsorption isotherm is shown in Figure 9, using eq 22 and reported data.[21] Stepwise adsorption is the outstanding feature of the isotherm, and this was simulated using adsorption of both A and $A_{n\times m}$ (A_{15}). To obtain the step by step adsorption, we found it necessary to exclude A_3, suggesting that successive steps will show when species generating them are very different in size. It is important to underline that the isotherm in Figure 9 could be simulated using the solution equilibrium alone. Such a proposition was used earlier to account for adsorption kinetics and other effects.[22]

Values of $-\Delta\overline{G}^0_{agg}/RT$ shown in Table 1 indicate that aggregation in all cases is a favorable event when compared to thermal energy. Of course, this is consistent with the low aggregation onset of asphaltenes.

HSP data from ref 15 are collected in Table 2, reproduced here for convenience. As shown in this table, for the A1−toluene pair, RED > 1, indicating that A1 is not soluble in toluene. This is coherent with aggregate formation at very low concentrations. Miscibility of the A1−A2 pair is predicted (RED < 1), as well as miscibility in toluene of the $A1_3$−$A2_5$ octamer aggregate (see Table 2).

DISCUSSION

Among the objectives of this work is to account for asphaltene aggregation using a mathematical model common to properties examined under similar conditions (toluene and room conditions). The good fittings shown above for properties examined suggest that we accomplished this goal. Thus, equilibrium formation in solution of relatively small aggregates

dx.doi.org/10.1021/ef200107k |Energy Fuels XXXX, XXX, 000–000

or nanoaggregates could describe the above properties in a concentration range covering 2−3 orders of magnitude in c_0.

In view of the very low solubility of the A1 fraction (about 90 mg L^{-1}, toluene, and room temperature[13]), the formation of nanoaggregates at very low concentrations is expected. Co-solubilization of these aggregates by A2 (second step) halt the phase separation that would follow otherwise.

The presence of maximum values in the simulation of both α_{LT} and β_T properties was close to corresponding experimental values, strongly suggesting that aggregation is a stepwise process similar to the one shown in eq 1. Moreover, because the number of molecules in aggregates is relatively small, the change in properties should be progressive rather than abrupt, as is the case when relatively large aggregates are formed.

Stepwise aggregation is consistent with the adsorption isotherms (see Figure 9) where, as described in Experimental Section, relative large aggregates, formed in solution and adsorbed at the interface, account for the measured stepwise adsorption isotherm.

Stepwise aggregation would in principle be observed when subsequent steps involve different species. Although for mathematical simplicity, the present model does not explicitly consider this to be the case, it does so implicitly by assuming different equilibrium constants in the first and second steps. Here, we propose that the first aggregation step involves the component of the low soluble fraction A1, which has a toluene−A1 RED > 1 and a very low toluene solubility (see above). The second step would be described as a solution mixing of A1 and A2, leading to a soluble colloid. RED < 1 for the A1−A2 pair warrants miscibility among them, and using the procedure described above (see the Experimental Section), a RED between the $A1_3$−$A2_5$ aggregate and toluene would be about 0.86 when three molecules of A1 and five molecules of A2 are used to built the aggregate (see Table 2). We also consider that aggregate A_{15}, used in adsorption experiments, would contain enough molecules of A2 to keep it in solution.

Accordingly, asphaltene colloids could be considered as an A1−A2 solid solution, which in turn is soluble in toluene. As expected, soluble A2 would be in an adsorption−desorption equilibrium between colloid and bulk, and in this case, the equilibrium would be controlled by the RED value corresponding to the pair colloid periphery media. In other words, the amount of A2 in the mixture, at the periphery, would be such that RED < 1 for the above pair.

Conceptually, the sequential aggregation described above based on very low solubility of A1, leading to aggregate formation, followed by co-solubilization of these aggregates by A2, avoiding phase separation at relatively low concentrations, is the foundation of the present model. A solubility test in more than 50 solvents shows that, in comparison to A2, the solubility of A1 is less, regardless of the solvent nature. Thus, in general, for solvents or media, in which asphaltenes are soluble and A1 is not, the present model is expected to hold.

The scope of the present model is limited to conditions similar to the one described above and is not intended to cover the general behavior of asphaltenes in crude oil reservoir (such as phase separation), Issues such as temperature and pressure dependence are not within the scope of the present model.

CONCLUSION

The mathematical model proposed on the basis of the two consecutive equilibrium steps was found consistent with reported experimental techniques dealing with asphaltene aggregation. The model was found coherent with nanoaggregate formation at extremely low concentrations (first step), which is consistent with equally extremely low solubility of asphaltene fraction A1. The addition to A2 aggregates of soluble fraction molecules (A2TM) in the second step keeps aggregates in solution, thus avoiding phase separation in toluene. The model, along with SP data, was found coherent with a two-step equilibrium mechanism, where A1TM of high SP and low toluene solubility forms aggregates in the first step and toluene-soluble A2TM is added in a second step to form a soluble colloid. Solubility of colloid would be warranted when enough A2TM, present at the colloid periphery, would keep the colloid media RED below 1. RED < 1 for the of A1−A2 pair warrants miscibility between them.

In short, the partition of A2TM, between insoluble phases (A1 and toluene), leads to a soluble colloid with interfacial tension $\gamma = 0$. For example, as a possible extension of the present ideas to crude oils, using a TEM technique, it was shown that extra-heavy oils have a very high concentration of the colloidal phase;[23] however, such oils show no flocculation tendency at all.

ASSOCIATED CONTENT

Supporting Information. Mass balance for equilibrium eq 1. This material is available free of charge via the Internet at http://pubs.acs.org.

AUTHOR INFORMATION

Corresponding Author
*E-mail: socrates.acevedo@ciens.ucv.ve.

ACKNOWLEDGMENT

The financial support provided by projects FONACIT (G2005000430) and CDCH (AI-03-12-5509-2004, PG-03-00-5732-2004, and PI-03-00-5648-2004) is gratefully acknowledged. We also thank Lic. Betilde Segovia for administrative assistance.

NOMENCLATURE

A1 = fraction of asphaltenes of low solubility and corresponding higher HSP; in particular, solubility in toluene is close to 0.1 g L^{-1} at room conditions
A2 = fraction of asphaltenes with solubility and HSP close to asphaltenes
A1TM = molecules present in fraction A1
A2TM = molecules present in fraction A2
As = asphaltenes
C or c = monomer concentration; C, molar units; c, mass units (g L^{-1} or mg L^{-1})
C_n = concentration of n aggregates (trimers in this work)
C_{n+m} = concentration of $(n + m)$ aggregates (octamers in this work)
C_0 or c_0 = total sample added to solution in the form of monomers; C_0, molar units; c_0, mass units
D = dispersion component in the HSP method
D_m = self-diffusion or rate of self-diffusion coefficients

DBPR = dual-beam photothermal reflection
$\Delta\overline{G}^{0}_{agg}$ = Standard aggregation molar free energy change corresponding to the formation of $m + n$ aggregates from monomers in toluene
H = hydrogen-bonding component of SP employed in the HSP method
HSP = Hansen solubility parameter
K_1 = equilibrium constant for the formation of n aggregates in toluene at room conditions
K_2 = equilibrium constant for the formation of $n + m$ aggregates in toluene at room conditions
M = molecular mass
M_n = number average molecular mass
RED = relative energy difference between components of a solution within the scope of the HSP method; RED values are used here as a miscibility criteria; when RED < 1, components are miscible and not miscible otherwise
R_0 = sphere radius in the HSP method
SP = solubility parameter
VPO = method for M_n determination using sample solutions above 1 g L^{-1} concentration
V_{US} = ultrasound velocity
$\Delta\alpha_{LT}$ = difference between heat diffusion coefficients for asphaltenes and resins
β_T = heat diffusion coefficient of asphaltenes in the DBPR technique
ν_C = amount of solute adsorbed at the toluene/silica interface

REFERENCES

(1) Speight, J. G. *The Chemistry and Technology of Petroleum*; Taylor and Francis Group: London, U.K., 2007; ISBN: 0849390672.
(2) Sheu, E. Y. In *Structures and Dynamics of Asphaltenes*; Mullins, O. C., Sheu, E. Y., Eds.; Plenum Press: New York, 1998; Chapter 4, p 115.
(3) Acevedo, S.; Rodríguez, P.; Zuloaga, C. *Energy Fuels* **2008**, *22*, 2332–2340.
(4) Sheu, E. Y.; De Tar, M. M.; Storm, D. A.; DeCanio, S. J. *Fuel* **1992**, *71*, 299–302.
(5) Acevedo, S.; Ranaudo, M. A.; Pereira, J. C.; Castillo, J.; Fernández, A.; Pérez, P.; Caetano, M. *Fuel* **1999**, *78*, 997–1003.
(6) Norinaga, K.; Wargardalam, V. J.; Takasugi, S.; Iino, M.; Matsukawa, S. *Energy Fuels* **2001**, *15*, 1317–1318.
(7) Andreatta, G.; Bostrom, N.; Mullins, O. C. *Langmuir* **2005**, *21*, 2728–2736.
(8) Evdokimov, I. N.; Eliseev, N. Y.; Akhmetov, B. R. *Fuel* **2006**, *85*, 1465–1472.
(9) Lisitza, N. V.; Freed, D. E.; Sen, P. N.; Song, Y. *Energy Fuels* **2009**, *23*, 1189–1193.
(10) Groenzin, H.; Mullins, O. C. *J. Phys. Chem. A* **1999**, *103*, 11237–11245.
(11) Jaimes, B.; Pulgar, D.; Ranaudo, M. A.; Chirinos, J.; Caetano, M. *Rev. Sci. Instrum.* **2010**, *81*, No. 024902.
(12) Durand, E.; Clemancey, M.; Lancelin, J. M.; Verstraete, J.; Espinat, D.; Quoineaud, A. A. *Energy Fuels* **2010**, *24*, 1051–1062.
(13) Gutiérrez, L. B.; Ranaudo, M. A.; Méndez, B.; Acevedo, S. *Energy Fuels* **2001**, *15*, 624–628.
(14) Acevedo, S.; Castro, A.; Negrin, J. G.; Fernández, A.; Escobar, G.; Piscitelli, V.; Delolme, F.; Dessalces, G. *Energy Fuels* **2007**, *21*, 2165–2175.
(15) Acevedo, S.; Castro, A.; Vásquez, E. ; Marcano, F.; Ranaudo, M. A. *Energy Fuels* **2010**, *24*, 5921–5933.
(16) Hansen, C. M. *Hansen Solubility Parameters. A User's Handbook*; CRS Press: Boca Raton, FL, 2000; ISBN 0-8493-1525-5.
(17) Acevedo, S.; Guzmán, K.; Ocanto, O. *Energy Fuels* **2010**, *24*, 1809–1812.
(18) Martinez-Haya, B.; Hortal, A. R.; Hurtado, P.; Lobato, M. D.; Pedrosa, J. M. *J. Mass Spectrom.* **2007**, *42*, 701–713.
(19) Zhang, Y.; Takanohashi, T.; Sato, S.; Saito, I.; Tanaka, R. *Energy Fuels* **2004**, *18*, 283–284.
(20) Acevedo, S.; Escobar, G.; Ranaudo, M. A.; Gutiérrez, L. B. *Fuel* **1994**, *73*, 1807–1809.
(21) Acevedo, S.; Castillo, J.; Fernández, A.; Goncalves, S.; Ranaudo, M. A. *Energy Fuels* **1998**, *12*, 386–390.
(22) Acevedo, S.; Ranaudo, M. A.; García, C.; Castillo, J.; Fernández, A.; Caetano, M.; Goncalves, S. *Colloids Surf., A* **2000**, *166*, 145–152.
(23) Acevedo, S.; Rodríguez, P.; Labrador, H. *Energy Fuels* **2004**, *18*, 1757–1763.